* http://www.apap-network.org

CALCULATION AND APPLICATION OF *R*-MATRIX ELECTRON-IMPACT EXCITATION DATA

GY Liang[1], N R Badnell[1], J R Crespo López-Urrutia[2], T M Baumann[2], G Del Zanna[3], P J Storey[4], H Tawara[2] and J Ullrich[2]

[1] Department of Physics, University of Strathclyde, Glasgow, G4 0NG, UK

[2] Max-Planck-Institüt für Kernphysik, Saupfercheckweg 1, Heidelberg, 69117, Germany

[3] DAMTP, Centre for Mathematical Sciences, Cambridge, CB3 0WA, UK

[4] Department of Physics and Astronomy, University College London, London, WC1E 6BT, UK

Ⅰ. Motivation: from astrophysical and fusion communities

— **Line identification:** A large amount of emission lines in EUV and X-ray regions were observed by spectrometers on space satellites (e.g. Hinode/EIS, Chandra, XMM-Newton) with high-resolution and high collection area.

— **Diagnostics:** Many emission lines detected by spectrometers show potential diagnostics of the n_e and T_e of coronal-like hot plasmas. Further detailed investigation of coronal structure and heating mechanism of hot-plasmas

— **Atomic physics:** Many available excitation data are from poor approximation (e.g. distorted-wave). More accurate method (R-matrix) and parallel computation are feasible now

Table 1: Level energy (Ryd) of S^{9+} from different calculation along with experimental value from NIST v3.

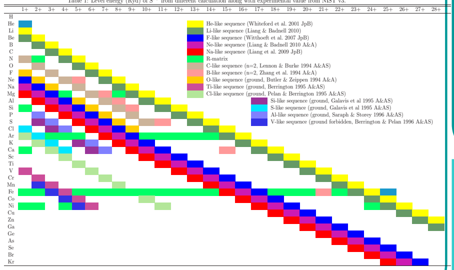

♦ *One of goals of UK APAP—Atomic Processes for Astrophysical Plasmas network*:* provides excitation data for iso-electronic sequence across an extensive range of astrophysically relevant elements within *R*-matrix framework

Ⅲ. Recent results as part of APAP network

For a summary of earlier work by the APAP Network , see our presentation in XXVI International conference on Photonic, Electronic and atomic collisions (ICPEAC 2009)[3]

A. *R*-matrix electron-impact excitation of Ne-like iso-electronic sequence[4]

Target configuration interaction (CI) is based on the configurations of [$1s^2$]$2s^22p^6$, $2s^22p^5\{3,4,5\}l$, $2s2p^6\{3,4,5\}l$, ($l \in$ s, p, d , f and g) $2s^22p^5\{6,7\}l'$, ($l' \in$ s, p and d) and $2s^22p^43l\{4,5\}l''$ ($l'' \in$ s, p, d , f and g)

(N+1)-system close-coupling (CC) is based on the configurations of [$1s^2$]$2s^22p^6$, $2s^22p^5\{3,4,5\}l$, $2s2p^6\{3,4,5\}l$, and $2s^22p^5\{6,7\}l'$ ($l' \in$ s, p and d)

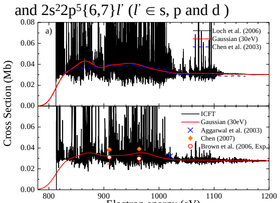

Original and convoluted (Guassian profile with a width of 30 eV) cross section of an important transition line $2s^22p^53d\ ^3D_1 \rightarrow 2s^22p^6\ ^1S_0$ (3D) of Fe^{16+} from different theoretical theoretical approaches and experimental measurement at electron beam ion trap (EBIT)

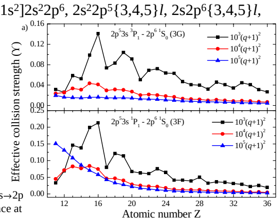

Effective collision strength of 3s→2p transition lines along the sequence at three temperatures

※ The excitation data are assessed in detail for ions spanning sequence, and confirmed to be a significant improvement than previous sequence data used extensively by modeling communities, e.g. astrophysical and fusion studies

※ A complicated structure of the effective collision strength along the iso-electronic sequence appears at low temperatures for those lines with strong resonances, which precludes interpolation in Z

C. *R*-matrix inner-shell electron-impact excitation for Li-like iso-electronic sequence with Auger and radiation damping[6]

The target CI and CC expansions are both taken to be 195 fine-structure levels (89 *LS* terms) of configurations: $1s^2\{2,3,4\}l$ and $1s2l\{2,3,4\}l'$

The resonance state configurations are of the form $1s[2s-4f]^2nl$ ($n \geq 5$) and they decay via the following channels:

$1s[2s-4f]^2\,nl \rightarrow 1s^2[2s-4f] + e^-$ (1)

$\rightarrow 1s^2nl + e^-$ (2)

$\rightarrow 1s^2[2s-4f]^2 + h\nu$ (3)

$\rightarrow 1s^2[2s-4f]\ nl + h\nu$ (4)

The participator KLn/KM*n*/KN*n* Auger and radiation pathways (1) and (3) are automatically described in the *R*-matrix method. However the spectator KLL/KLM/KLN Auger and radiation pathways (2) and (4) are independent of *n* and only low-*n* resonances ($n \leq 4$ here) can be included in the normal close-coupling expansion. The ICFT method easily takes account of the damping pathways (1)—(4) *via* an optical potential.

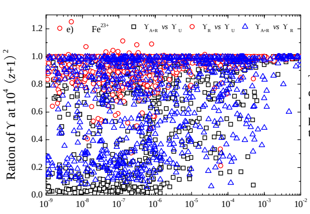

The ratio of effective collision strengths between that with radiation or Auger-plus-radiation damping and that without damping

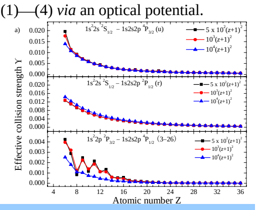

Effective collision strength (ϒ) of inner-shell transition lines along the Li-like iso-electronic sequence at three temperature

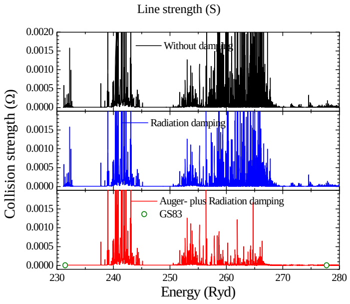

Collision strengths calculated with ICFT *R*-matrix method without damping, and with radiation damping or Auger-plus-radiation damping for one transition of Ar^{15+}

※ Resultant effective collision strengths are assessed to be a significant improvement than previous calculations and reliable for ions with charge higher than 5 along the sequence

※ The enhancement of ϒs from resonances in Ω decreases with increasing of the nuclear charge Z because of the Auger-radiation damping effects for a given transition

※ The Auger-radiation damping is more significant and widespread for more transitions with increasing Z, although the radiation damping effect increases

※ The complicate structure appears from some excitations as shown in other sequence calculations

※ An independent calculation for valence-electron excitations up to levels of n =5 complexes has been done along the sequence to generate a self-consistent dataset, which is also assessed to be reliable

Ⅱ. Method

♦ Radial wave-functions are generated by uisng AUTOSTRUCTURE

♦ *R*-matrix instead of distorted-wave (DW) method was adopted here, which efficiently takes resonances in electron-ion interaction into account

♦ Intermediate-coupling frame transformation (ICFT)[1] *R*-matrix instead of Breit-Pauli and fully relativistic Dirac (DARC) method

Advantages:

1. Less-time demanding: consider *LS*-coupled Hamiltonian
2. Eliminates at root the deficiency of previous *LS*-based methods (e.g. JAJOM) via use of multi-channel quantum defect theory (MQDT)
3. Has comparable accuracy with other two kinds of *R*-matrix methods [1]
4. Auger and radiation damping via spectator electron ($n \geq 3$, 4 or 5) pathways can easily be taken into account via a optical potential [2]
5. Current ICFT code has been parallelized and has shown to be highly robust

B. *R*-matrix electron-impact excitation data for Al-like Fe[5]

The target CI expansion is taken to be the 2985 fine-structure levels (1241 *LS* terms) belonging to the configurations of $3s^x3p^y3d^z$ (x+y+z=3), $3s^24l$, $3s3p4l$, $3p^24l$, $3p3d4l$, $3d^24l$, $3l4l'4l''$ and $3l3l'5l''$

The (N+1)-system CC expansion is based on the 197-levels of configurations $3s^x3p^y3d^z$ (x+y+z=3), $3s^24l$, $3s3p4$\{s, p and d\}

a. 40 continuum basis per orbital angular momentum.

b. The contribution from partial waves up to J=12 included electron-exchange.

c. The contribution from higher partial waves up to J=42 were included via a non-exchange calculation; then a "top-up" was used to include the contribution from higher J-values.

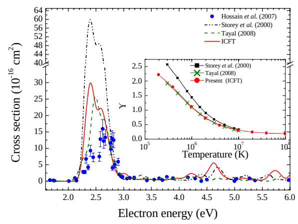

Cross section of the coronal green line of different *R*-matrix calculations along with the laboratory measurement. Inset panel shows the resultant effective collision strength over temperatures

Ratio of effective collision strengths at three temperatures between the present ICFT *R*-matrix calculation and previous small-scale calculations

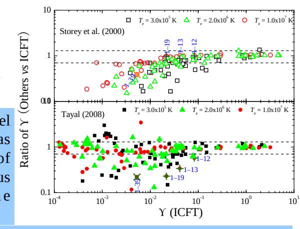

※ Comparison of level energies, *gf*-values as well as life-times of excited levels give us confidence to the excitation data

※ The excitation data is assessed to be reliable, and a significant improvement is obtained via a larger CI expansion in target and larger CC expansion to consider resonances attached to the levels of $3s^24l$ and $3s3p4l$ ($l \in$ s, p and d) configurations

D. Modeling and diagnostic with the new updated atomic data for spectroscopy of hot astrophysical and laboratory plasmas[5,7]

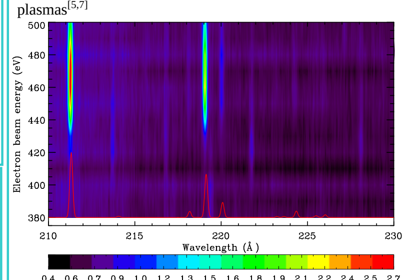

2D representation of spectra of Fe ions as a function of electron beam energy, conducted at Heidelberg electron beam ion trap (Germany)

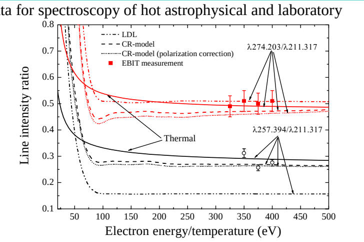

Intensity ratios of EUV transition lines of Fe XIV at thermal and Gaussian electron-energy distributions, as well as laboratory measurements. Polarization effect due to non-thermal electrons is also illustrated.

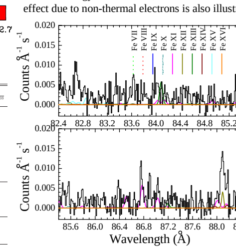

Soft X-ray spectra in Procyon *Chandra* LETGS observations and theoretical modeling by using newest R-matrix excitation data and part of DW results

Table 2: Observed branching ratios and electron-density-insensitive line intensity ratios of EUV lines for different observations

	Branching ratio λ220.084/λ211.317	λ252.199/λ264.789	λ257.394/λ270.520	λ289.150/λ274.203	λ356.645/λ334.178	line ratio λ274.203/λ211.317	λ334.178/λ274.203	λ444.219/λ334.178	λ270.520/(λ264.789+λ274.203)
Observations									
SERTS – 89	0.25 ± 0.07	0.18 ± 0.06	0.38 ± 0.09	0.072 ± 0.024	0.028 ± 0.010	1.01 ± 0.18	0.62 ± 0.10	0.018 ± 0.005	0.24 ± 0.04
BFS08 – QS		0.20	0.42	0.040		0.55			0.23
BFS08 – AR1		0.18	0.53	0.048		0.46			0.24
BFS08 – AR2		0.20	0.62	0.042		0.44			0.22
BFS08 – Limb		0.21	0.50	0.054		1.76			0.27
BFS08 – Limb + 20″		0.19	0.53	0.040		1.10			0.26
Present – QS off Limb		0.21^a	0.71	0.100^b		0.40^b			0.23^b
Present – AR		0.20^a	0.52	0.050^b		0.46^b			0.26^b
Present – high n_e		0.21^a	0.54	0.050^b		0.46^b			0.23^b
MH73	0.28	0.26		0.060		0.60			0.26
Laboratory (EBIT) measurements									
E_e = 325 eV	0.23 ± 0.07	0.12 ± 0.07^c	0.57 ± 0.14^d			0.49 ± 0.09			0.20 ± 0.03
E_e = 350 eV	0.17 ± 0.03	0.20 ± 0.03^c	0.55 ± 0.06^d			0.51 ± 0.08			0.20 ± 0.02
E_e = 375 eV	0.15 ± 0.02	0.22 ± 0.03^c	0.61 ± 0.05^d			0.50 ± 0.08			0.19 ± 0.03
E_e = 400 eV	0.17 ± 0.02	0.21 ± 0.03^c	0.58 ± 0.04^d			0.51 ± 0.08			0.20 ± 0.02
Theory									
BRS95	0.22	0.23	0.71	0.095	0.038	0.37	0.63		0.35
YLT98	0.21	0.24	0.74	0.089	0.036	0.35 ± 0.03	0.69 ± 0.07	0.015 ± 0.002	
SMY00	0.22	0.24	0.66	0.061	0.029	$0.53^{+0.05}_{-0.03}$	$0.64^{+0.06}_{-0.04}$	$0.028^{+0.011}_{-0.009}$	$0.26^{+0.02}_{-0.01}$
Present	0.21	0.24	0.70	0.076	0.032	0.55	0.70	0.032	0.26

※ Laboratory measurement benchmark the theoretical modeling and astrophysical observations

※ The present model satisfactorily explains the spectra of Fe XIV in solar observations, and identify some lines

※ Some emission lines from highly-charged iron ions are identified firstly in Procyon observations

Ⅳ. Summary

— An extensive set of reliable excitation data is being generated under the APAP project

— This will update much of DW data (via CHIANTI[8]) presently used by astrophysical community and its use may overcome some shortcomings in astrophysical modelling;

— This is also of importance to fusion modelling and diagnostics *via* updates of the ADAS[9] database

— Laboratory benchmark (via EBIT) is necessary for theory and astrophysical analysis

References

[1] Griffin D C, Badnell N R and Pindzola M S 1998 *J.Phys. B: At. Mol. Opt. Phys.* **31** 3713

[2] Robicheaux F, Gorczyca T W, Pindzola M S, Badnell N R 1995 *Phys. Rev.* A **52** 1319

[3] Liang G Y, Badnell N R, Storey P J, Whiteford A D, Del Zanna G 2009 *J.Phys.: Conference series* **194** 062006

[4] Liang G Y and Badnell N R 2010 *Astro. & Astrophys.* **518** A64

[5] Liang G Y, Badnell N R, Crespo López-Urrutia J R, Baumann T M, Del Zanna G, Storey P J, Tawara H and Ullrich J 2010, ApJS (in press)

[6] Liang G Y and Badnell N R 2010 (draft finished)

[7] Liang G Y and Zhao G 2010, *MNRAS* **405** 1987

[8] Landi E, Del Zanna G, Young P R, Dere K P, Mason H E and Landini M 2006 *Astrophys. J. Supp. Ser.* **162** 261

[9] Summers H P 2004 *The ADAS User manual version 2.6* http://www.adas.ac.uk